Biochemical and Biophysical Research Communications **258,** 102–108 (1999)
Article ID bbrc.1999.0592, available online at http://www.idealibrary.com on IDEAL®

Dynamics of DNA Molecules in Gel Studied by Fluorescence Microscopy

Ronald M. Kantor, Xuan-Hui Guo, Edward J. Huff, and David C. Schwartz[1]
W. M. Keck Laboratory for Biomolecular Imaging, Department of Chemistry, New York University, New York, New York 10003

Received March 22, 1999

The dynamics of individual DNA molecules in a thin gel were studied with fluorescence microscopy. Driven by an electric field, molecules hooked around isolated obstacles and became extended. By analyzing molecular images, we identified the reptation tube and primitive chain. When the field was turned off, the molecules relaxed. The relaxation time τ_1 and primitive chain length $\langle L\rangle$ at equilibrium depend on N, the size of the molecule in base pairs, consistently with reptation theory. Using five yeast chromosomal DNAs ranging in size from 245 kb to 980 kb, we found that:

$$\langle L\rangle(\mu\text{m}) = 0.0749[N/1000] - 6.94$$

$$\tau_1(\text{sec}) = 0.017[N/1000]^{1.45} \quad [1]$$

These results constitute a way of sizing individual DNA molecules by imaging rather than by gel electrophoresis.

Quicker DNA mapping and sequencing rate would expedite the human genome project. Physical mapping involves measuring the sizes of DNA molecules or fragments. Among today's techniques for sizing large DNA molecules, pulsed field gel electrophoresis (PFGE) is most popular (1-3). PFGE sizes molecules by comparing their electrophoretic mobilities with those of co-running standards, such as λ-bacteriophage DNA concatamers. Size standards are needed because the absolute mobility of a molecule depends on gel concentrations, pulse times, and other experimental conditions. Other reported approaches include the viscoelastic technique (4) and electron microscopy (5), which have many physical limitations.

To find a new way of quickly sizing large single DNA molecules, we have developed OCM, or optical contour maximization (6-9). In OCM, a DNA molecule in the interface between an agarose gel and a glass coverslip first is stretched by an electric field and then, as it relaxes, imaged by fluorescence microscopy. The images are analyzed to measure the primitive chain contour length $L(t)$ of the molecule as a function of time. The process is repeated many times in order to emulate a thermodynamic ensemble of such molecules. Late in the relaxation process, the ensemble average contour length $\langle L(t)\rangle$ should obey

$$\langle L(t)\rangle = \langle L\rangle + A\ \exp(-t/\tau_1) \quad [2]$$

Since the equilibrium length $\langle L\rangle$ is proportional to N, the size of the molecule in base pairs, while the relaxation time τ_1 varies as a power of N, there should be two ways of obtaining N from $\langle L(t)\rangle$.

THEORETICAL DEVELOPMENT

Reptation model of DNA in a gel. Consider an individual DNA molecule embedded in a gel. The rigid mesh of gel fibers, spaced an average distance a apart, constrains the molecule. Conformations accessible to the molecule belong to two broad categories: simple conformations, where the molecule always remains within an imaginary tube of radius a, and branched conformations, where at one or more places the molecule kinks out a distance $h > a$, doubles back on itself, and returns to its original path. A kink of size $h < a$ is known as a 'defect' or 'repton' (10). Simple and branched conformations are illustrated in Figs. 1A and 1B, respectively.

DeGennes has shown that kinking costs entropy proportional to h/Λ (11) where Λ, the persistence length, is about 50nm for DNA (12). Thus a branched conformation always lies within a narrow channel in the space of accessible conformations. A molecule in a simple conformation should take many tube disengagement times τ_D to reach a branched conformation (10). $\tau_D \propto N^3b^4/kTa^2$, where b, the separation between successive base pairs, averages 0.34 nm, k is Boltzmann's constant, and

[1] To whom reprint requests should be addressed. Fax: 212-995-4681. E-mail: d.c.schwartz@nyu.edu.

0006-291X/99 $30.00

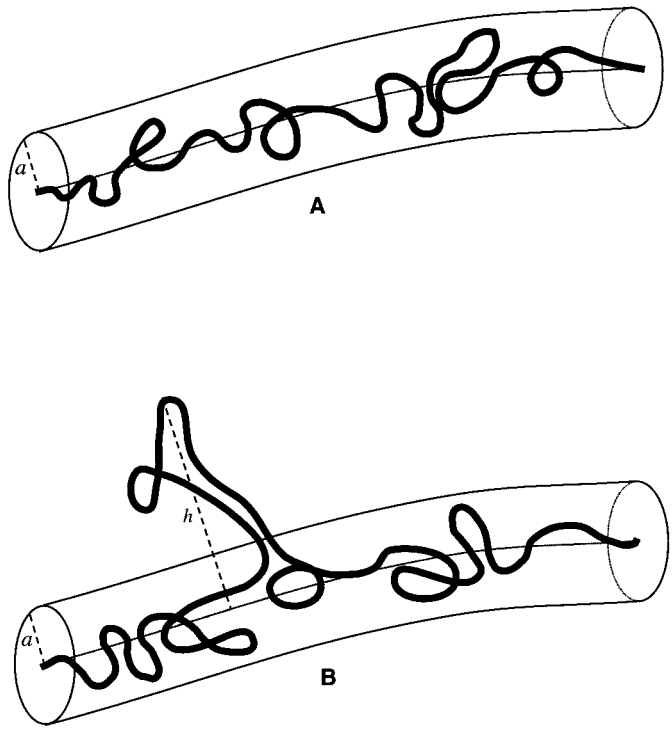

FIG. 1. Cartoons of a polymer embedded in a gel. (*A*) Simple conformation. (*B*) Branched conformation.

T temperature. For large molecules, τ_D is much longer than the linear relaxation times τ_m defined below.

While any particular branched conformation is hard to reach, branched conformations collectively dominate the thermal equilibrium distribution. Since a large polymer in a gel reaches branched conformations slowly, the polymer should take a very long time to reach thermal equilibrium. Zimm and others (13) argue that over times sufficiently long compared to τ_D, such a polymer will collapse to an isotropic random coil. For a multi-kilobase DNA embedded in an agarose gel to collapse may take many years.

On the shorter time scales relevant to our experiments, we can assume that the gel always confines DNA molecules to tubular domains. This fundamental assumption of deGennes' reptation model (11, 14, 15) permits the partition function of a molecule to be factored (10)

$$Z_{dG} = \int dL\Omega(L)z(L) \quad \text{where} \quad \Omega(L) \propto \exp(3L/a) \qquad [3]$$

is the number of distinct tubes of length L that can fit through the mesh, and $z(L)$ is the partition function of a molecule confined to one such tube. If $Nb \gg \Lambda$, the molecule may be modeled as a random flight of $\tilde{N}$ steps of length $\tilde{b}$, where $\tilde{b} \approx 2\Lambda$ and $\tilde{N}\tilde{b} = Nb$. Then

$$z(L) \propto \exp(-3L^2/2\tilde{N}\tilde{b}^2) \qquad [4]$$

and the contour length at thermal equilibrium is evaluated straightforwardly

$$\langle L \rangle = Z_{dG}^{-1} \int dL\Omega(L)z(L)L = \tilde{N}\tilde{b}^2/a \qquad [5]$$

as is the variance in L:

$$\langle \Delta L \rangle^2 = Z_{dG}^{-1} \int dL\Omega(L)z(L)(L - \langle L \rangle)^2 = a\langle L \rangle/3 \qquad [6]$$

When DNA is highly concentrated, mutual entanglement of molecules should constrain each molecule's movement as would a gel (10). Under such conditions, the reptation model should also apply. By manipulating single, fluorescently labeled molecules with optical tweezers, Perkins (16) has observed tube-like motion of entangled DNA molecules.

The reptation model of DNA has been verified in both constant and pulsed field gel electrophoresis, and in DNA migrating through two-dimensional microlithographic arrays (17, 18). Reptation approximates well the behavior of DNA molecules smaller than 100 kb (19, 20). Reptation is somewhat less accurate for larger molecules, which are more easily driven out of the tube (21-25). Nevertheless, the model should be valid for long DNA molecules in the absence of an applied electric field.

Dynamics of free DNA in solution. To understand the dynamics of a DNA molecule in a gel, it is useful first to examine the dynamics of DNA free in solution. By chemically fixing one end of a DNA molecule and attaching the other end to a magnetic bead, Smith et al. (26) measured the mean end-to-end distance $\langle x \rangle$ as a function of applied force F. Bustamante et al. (27) found an approximate analytical relation between the fractional extension of the molecule $\epsilon \equiv \langle x \rangle / Nb$ and F:

$$\frac{\Lambda}{kT} F \approx \frac{1}{4}\left[\frac{1}{(1-\epsilon)^2} - 1\right] + \epsilon \qquad [7]$$

The nonlinear part of F grows with ϵ. Define

$$\phi(\epsilon) \equiv \left(\frac{2\Lambda}{3kT}\frac{F}{\epsilon}\right) - 1 \qquad [8]$$

to be the fractional excess over linear restoring force.

If ϕ is small, the molecule may be modeled using linear forces. In the Rouse model (28), a molecule is represented by a series of $\tilde{N}$ beads at positions $\{\vec{r}_0, \ldots, \vec{r}_{\tilde{N}-1}\}$, each having coefficient of friction ζ with solvent and interconnected by Hookean forces

$$\vec{f}_{i,i+1} = \frac{-\partial}{\partial(\vec{r}_{i+1} - \vec{r}_i)} V_{\mathrm{H}} \quad \text{where}$$

$$V_{\mathrm{H}} \equiv \frac{3}{2}\frac{kT}{\tilde{b}^2}\sum_{i=0}^{\tilde{N}-1} |\vec{r}_{i+1} - \vec{r}_i|^2 \qquad [9]$$

The dynamics of a Rouse chain are a superposition of normal modes $\{m | 1 \le m \le \tilde{N}\}$ which decay with lifetimes (29) τ_m. For small m and large $\tilde{N}$,

$$\tau_m \approx \frac{1}{3\pi^2}\frac{\tilde{b}^2\zeta}{kT}\left(\frac{\tilde{N}}{m}\right)^2 \qquad [10]$$

The Zimm model (30) approximates solvent-mediated interactions among the beads with long-range pairwise potentials. In Zimm's model (30), the chain has a similar spectrum of modes, but with lifetimes

$$\tau_m \propto \frac{\tilde{b}^2\zeta}{kT}\left(\frac{\tilde{N}}{m}\right)^{3/2} \qquad [11]$$

Dynamics of DNA in OCM. At the interface with the coverslip, the gel used in OCM is a loose mesh a few μm deep, just dense enough to ensnare DNA molecules. At greater depths, the gel reaches its normal density. Denser gel below confines DNA to the interface. Sparse gel in the interface offers little resistance to DNA moving parallel to the coverslip. Nonetheless, as Fig. 2 shows, the interface gel does confine a DNA molecule to a reptation tube.

In OCM, an electric field is used to manipulate a DNA molecule in the interface. As soon as the molecule gets significantly extended, the electric field is removed, allowing the molecule to relax. If the primitive chain length L of the molecule is short enough that $\phi(L/Nb) \ll 1$, a Rouse or Zimm model can describe the relaxation process. The Hookean potentials Eqs. [9] can be separated into contributions along and transverse to the reptation tube:

$$V_{\mathrm{H}} = \frac{3}{2}\frac{kT}{\tilde{b}^2}\sum_{i=0}^{\tilde{N}-1}(s^{\parallel}_{i+1} - s^{\parallel}_i)^2 + \frac{3}{2}\frac{kT}{\tilde{b}^2}\sum_{i=0}^{\tilde{N}-1}|\hat{s}^{\perp}_{i+1} - \hat{s}^{\perp}_i|^2 \qquad [12]$$

Here, $s^{\parallel}$ is the axial coordinate and $\hat{s}^{\perp}$ are the two local transverse coordinates. Since the molecule is confined to a reptation tube, transverse modes cannot be excited significantly. From the expressions for the normal modes (30), we see that $L(t) = (s^{\parallel}_{\tilde{N}(t)} - s^{\parallel}_0(t))$ varies with time only in longitudinal modes with m odd. Stretching the molecule with an electric field excites these odd-ordered, longitudinal modes. After the field is turned off, each mode will decay according to its characteristic lifetime τ_{2n+1}. As relaxation nears completion, the mode $m = 1$, which has the longest lifetime, dominates, so that Eq. [2] holds.

MATERIALS AND METHODS

Materials. Yeast chromosomal DNA was resolved by Pulsed Oriented Electrophoresis (21) in 1% Seakem low melting agarose (FMC), 1/2× TBE (42.5 mM Tris, 44.5 mM boric acid, 1.25 mM disodium EDTA). Excised gel bands were equilibrated repeatedly in TE (10 mM Tris, 1 mM EDTA, pH 8.0) (31). Bands were equilibrated further in TE containing 10 mM NaCl, melted at 72°C for 10-15 min and cooled to 37°C. Ethidium bromide (final concentration 1 μg/mL) and 2-mercaptoethanol (final concentration 10 μg/mL) for minimizing photodamage (32) were added to the melted sample, which was maintained at 37°C from 10 min to a few hours. Using a cut-off yellow pipette tip, 10 μL of the sample was placed on a preheated slide with 1.8 cm × 1.8 cm coverslip in a staged electrophoresis chamber with 2 cm electrode spacing (21). The edges were sealed with mineral oil to prevent evaporation. Coverslips and slides were cleaned by boiling in 0.075 M HCl for one hour, rinsed with distilled water several times, and stored in 100% ethanol before use. Mounted samples were incubated at 4°C for at least 15 min before image collection at 37°C.

Instrumentation. A Zeiss Axioplan epifluorescence microscope was used with filter cube #15 (green excitation, red observation), and Pol Plan-Neofluar 100 × 1.30 numerical aperture objective. The distance per pixel was calibrated using the USAF-1951 resolution target and determined to be 0.217 μM. A 6115A precision power supply (Hewlett-Packard) was used to provide potential across the chamber electrodes. Frames from a C2400-SIT camera (Hamamatsu) were averaged by PixelPipeline (Perceptics), digitized (480 × 512 × 8 bits) and stored in a Macintosh IIfx computer. Averaged images were processed later to remove background, reduce noise, and simulate shadowing using NIH Image (http://rsb.info.nih.gov/nih-

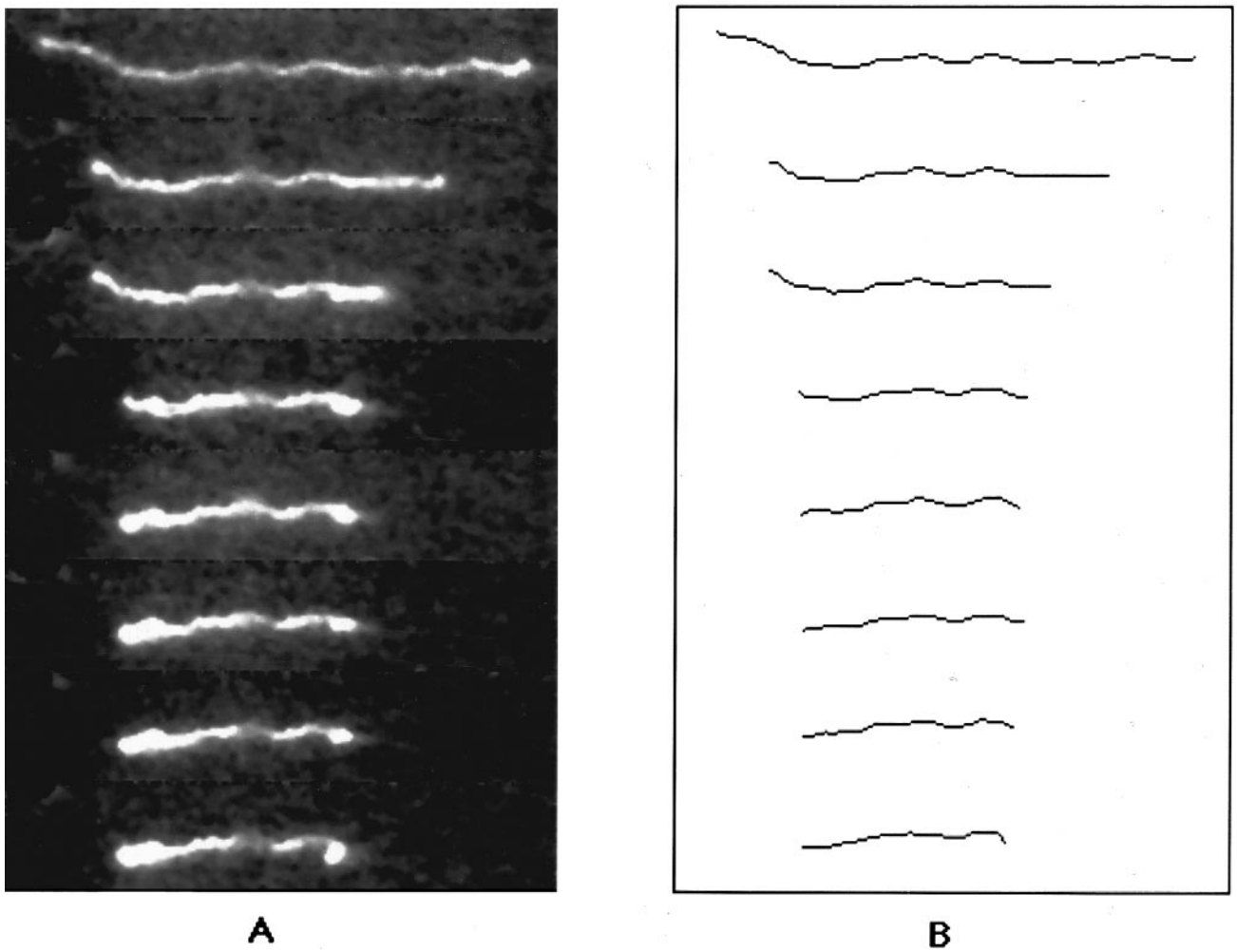

FIG. 2. A DNA molecule undergoing relaxation, after being stretched according to the experimental procedure described in the text. (*A*) Consecutive digital images. (*B*) Primitive chains determined by performing enhancement operations on the images in A.

image/) and NCSA Image (http://www.ncsa.uiuc.edu) software for Macintosh, and photographed by a film recorder (Polaroid).

Methods. A common phenomenon facilitates making digital images of DNA in a gel which permit quantitative comparison with reptation theory. DNA molecules in gels often become hooked around obstacles when driven by an applied electric field (21, 24, 33, 34). The 'arms' of such a hook extend as the molecule aligns with the electric field. The arms, of course, are never exactly equal in length. Since the force of the electric field is greater on the longer arm, the molecule quickly slides off the obstacle. At the moment that the molecule has slid off, it is significantly extended and roughly straight. The ends and reptation contour of the molecule then may be imaged readily. Since this extended conformation is disfavored thermodynamically, the molecule will begin to relax as soon as the field is turned off. Here we summarize our procedure for measuring this relaxation:

1. Locate a molecule under the microscope and bring it into focus.
2. Impose an electric field on a selected molecule and keep that molecule in view by alternating the direction of the field. Move the molecule back and forth until it becomes hooked around an obstacle. As soon as the molecule slides off the obstacle, turn off the electric field. If the whole molecule is still in the focal plane, start collecting images immediately.
3. Collect images at times t_i 10 or 20 seconds apart, averaging every 8 or 16 frames to obtain a total of up to 50 images.
4. Repeat steps 2 and 3 for a given molecule as many times as possible.
5. Analyze and process (reduce noise, smooth, threshold and skeletonize) each set of images with a program written in the macro-programming language of NIH Image. Measure the primitive chain lengths $L(t_i)$.
6. Average all the relaxation curves for a given molecule to approximate a thermal ensemble. Determine $\langle L \rangle$ from the final plateau of the relaxation curve and fit the curve to Eq. [2] to obtain τ_1.

RESULTS AND DISCUSSION

Reptation. In Fig. 2A, we present a typical set of images showing the relaxation of a 345 kb DNA molecule that had been subjected to the above procedure. The images confirm the assumptions of the reptation model, i.e. that the molecule is constrained to a tubular domain and retracts along its own contour. The reptation tube can be inferred from the trajectory of the molecule and the axis of the primitive chain can be resolved by image processing. As an example, we performed threshold, skeleton and analysis operations on the images in Fig. 2A, and present the results in Fig.

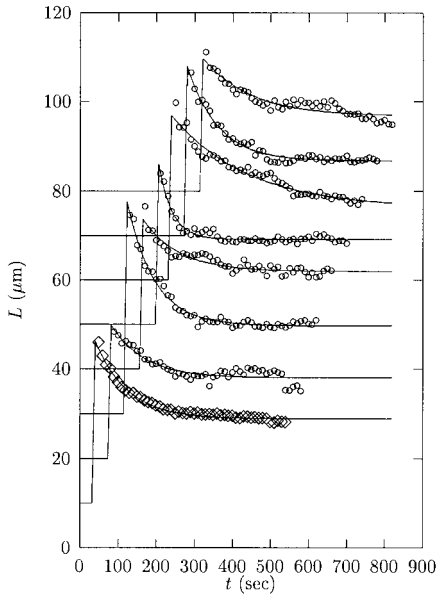

FIG. 3. Relaxation curves and fitted parameters obtained for seven OCM measurements made on a single molecule. The y-axis represents the contour length in μm and the x-axis the time in seconds. Experimental points are represented by empty circles, and the average by empty diamonds. The solid lines are nonlinear least squares fits to Eq. [2]. Each successive plot is offset by 50 sec horizontally and 10 μm vertically for clarity. The solid lines indicate the zero length and the zero time for each plot.

2B. In this manner, it is straightforward to determine the length of the primitive chain at various times.

Relaxation. The relaxation process was recorded seven times for the same 345 kb DNA molecule. Figure 3 shows plots of length versus time and Table 1 other quantities derived from each of these recordings. As the second column of the table indicates, $\epsilon = L(t_0)/Nb$, the fractional extension at the beginning of the process, ranged from 0.24 to 0.38, averaging 0.31. Correspondingly, $\phi(\epsilon)$, the fractional excess over linear restoring force, averaged 0.26 at the beginning of relaxation.

For each relaxation, $\langle L \rangle$ was estimated by averaging $L(t_i)$ over the last 15 time points. The results are listed in the last column of Table 1. The distribution in $\langle L \rangle$ is relatively narrow, with standard deviation $\langle \Delta L \rangle$ about 10% of the average $\langle L \rangle$. To our knowledge, this is the first direct measurement of the length of the primitive chain for DNA at equilibrium in a gel.

The relaxation time τ_1 was estimated by fitting a curve of the form Eq. [2] to $L(t_i)$ at the first 20 or 30 time points and $\langle L \rangle$. The third column of Table 1 lists the values obtained for each relaxation. The distribution in τ_1 is quite broad, with standard deviation around 50%. Part of this imprecision was due to the nonlinear part of the restoring force, which, as column two of Table 1 shows, varied with each relaxation.

A more important source of error, however, probably was variation in frictional forces. Each time the DNA molecule relaxed, it moved through a different area of the gel-coverslip interface, encountering a different set of obstacles. During the course of each relaxation, the frictional forces between the molecule and the gel were changing as the molecule made and lost contacts with gel fibers. This variation of friction with time depended on exactly where in the interface the molecule happened to be. As a result, the detailed course of relaxation with time likewise depended on the exact location of the molecule.

The value for τ_1 shown in the eighth row of the fourth column of Table 1, is the average of the values shown in rows one through six. The value for τ_1 given in the ninth row was obtained by calculating an average time-course for all seven relaxations

$$\bar{L}(t_i) = \frac{1}{7} \sum_{J=1}^{7} L_J(t_i) \qquad [13]$$

and then fitting a curve of the form Eq. [2] to $\bar{L}(t_i)$. Because such time point by time point averaging

TABLE 1

Relaxation Time and Equilibrium Length for a 345 kb DNA

Measurement	$\epsilon = L(t_0)/Nb$	$\phi(\epsilon)$	τ_1 (sec)	$\langle L \rangle$ (μm)
1	0.24	0.17	86 ± 13	18.0
2	0.38	0.37	72 ± 3	19.7
3	0.31	0.26	93 ± 11	21.9
4	0.29	0.23	35 ± 2	19.1
5	0.34	0.30	198 ± 21	16.3
6	0.31	0.26	79 ± 4	16.7
7	0.27	0.21	124 ± 17	16.7
Average*	0.31	0.26	98	18.4
Average†	0.31	0.26	83 ± 3	18.9
Std. Dev.	0.046	0.065	51	2.0

* Here, $L(t_0)/Nb$, τ_1, and $\langle L \rangle$ were obtained by fitting to each relaxation curve, and then averaged.

† Here, all relaxation curves were averaged, then $L(t_0)/Nb$, τ_1, and $\langle L \rangle$ were obtained by fitting to the averaged curve.

TABLE 2

Comparison of Measurements among Samples

Sample	Relaxations Recorded	τ_1 (sec)	$\langle L \rangle$ (μm)
1	3	78	19.1
2	8	114	19.1
3	4	102	18.0
4	5	133	18.9
5	5	97	20.8
Average		105	19.1
Std. Dev.		20.4	1.0

should cancel out location-dependent variations in the detailed course of relaxation, it should yield a more accurate value for τ_1.

Reproducibility. Sample preparation involves melting and cooling a small piece of gel. The procedure for gelation of agarose in a thin region between a slide and a coverslip is rather complicated (7). We found that experiments using different samples of the same kind of DNA give consistent results when the gels are well-formed and extra water on the gels has been removed.

The results of such a set of experiments are presented in Table 2. For each sample, the relaxation of a molecule was recorded a number of times. The relaxations were aggregated to generate an averaged relaxation time course. The values for τ_1 and $\langle L \rangle$ listed in columns three and four, respectively, were found by fitting a curve to the averaged time course. The distribution in τ_1 among the samples is much narrower than that obtained above, using a single sample but without such time point by time point averaging. The standard deviation $\langle \Delta L \rangle$ and $\Delta\tau_1$ are listed in row seven of Table 2.

Sizing yeast chromosomes. We performed relaxation measurements on DNAs from five different yeast chromosomes: (I) 245 kb, (VI) 280 kb, (III) 345 kb, (XI) 680 kb, (XIII) 980 kb. All of these molecules exhibited the anticipated relaxation behavior. Figure 4 shows

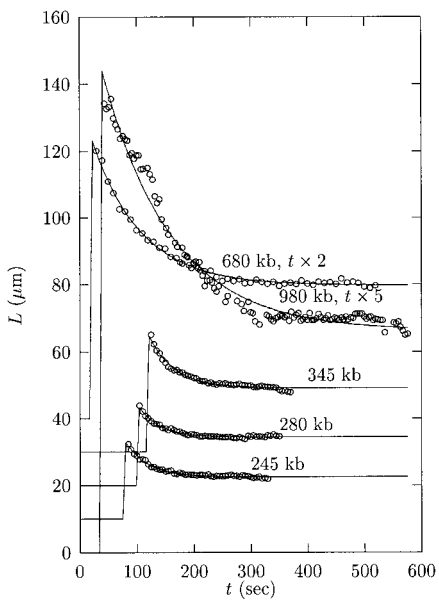

FIG. 4. Averaged relaxation curves and fitted parameters for five DNA molecules from *Saccharomyces cerevisiae* (36). As in Fig. 3, the solid lines are nonlinear least squares fits, and each line includes an indication of the zero time and zero length offset for the plot. Successive curves represent chromosome I (N = 245 kb), chromosome VI (N = 280 kb), chromosome III (N = 345 kb), chromosome XI (N = 680 kb), chromosome XIII (N = 980 kb). Each plot is offset by 20 sec horizontally and 10 μm vertically for clarity. The 680 kb molecule is plotted against time ÷ 2 (full scale is 1200 sec) and the 980 kb molecule is plotted against time ÷ 5 (full scale is 3000 sec).

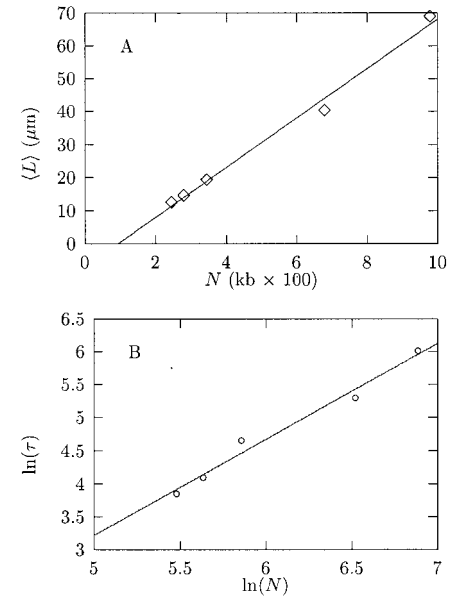

FIG. 5. Correlation of $\langle L \rangle$ and τ_1 with N based on data given in Fig. 4. Solid lines indicate linear least squares fit. Symbols are data points. (*A*) Plot of equilibrium length $\langle L \rangle$ versus N. (*B*) Plot of relaxation time τ_1 versus molecular size N.

therelaxation curves for these DNAs and the $\langle L \rangle$ and τ_1 values obtained by nonlinear least-squares fitting.

Figures 5A and 5B are plots of $\langle L \rangle$ and τ_1 versus molecular size N respectively. In keeping with theoretical expectation, we performed a linear fit of $\langle L \rangle$ to N and a log-log fit of τ_1 to N and obtained Eqs. [1]. That the fit of $\langle L \rangle$ to N has a negative intercept probably reflects the failure of the reptation model for short DNA molecules. A molecule whose fully extended length Nb is not too great compared to the mesh spacing a will not be restricted significantly by the gel. Such a molecule should behave as a self-avoiding random coil. Properly then, $\langle L \rangle$ should change from being proportional to N for large N to varying as N^{ν}, where the Flory exponent ν (11) is about 3/5, in the limit of small N. The good quality of the fit in Fig. 5B shows that τ_1 is an accurate, if imprecise, means of measuring size. Indeed, τ_1 should be a particularly useful measure, because it is more sensitive to small changes in N than is $\langle L \rangle$.

Zimm chain. That the exponent 1.45 in the fit Eqs. [1] of τ_1 to N is closer to the exponent 3/2 which appears in Eq. [11] than the exponent 2 in Eq. [10] suggests that a DNA molecule in an OCM gel should be modeled by a Zimm chain rather than a Rouse chain. Heretofore we have assumed that the gel network screens out solvent-mediated long-range interactions among chain segments. As noted above, however, OCM uses a relatively loose gel, which may not block all such interactions. Using optical tweezers to hold individual DNA molecules in a flowing solvent, Perkins et al. (35) also have measured the relaxation spectra of DNA. They

found that τ_1 varies as $\langle L \rangle^{\lambda}$, with $\lambda = 1.65 \pm 0.13$. Since $\langle L \rangle \propto N$, their results are nearly in agreement with ours.

In summary, we have presented a new technique for observing the dynamics of DNA molecules in a gel directly. The primitive chain can be seen easily and quantified by computer image processing. The relaxation time τ_1 and equilibrium length $\langle L \rangle$ depend on N, the size of the molecule, in a manner consistent with reptation theory. This study potentially provides a new approach for measuring the size of a DNA molecule or fragment by means of fluorescence microscopy.

ACKNOWLEDGMENTS

We thank X. Li for providing the images of yeast chromosome XIII (980 kb), and S. Ramnarain, L. Hernandez, I. Maity and M. Hsu for technical assistance.

REFERENCES

1. Schwartz, D., Saffran, W., Welsh, J., Haas, R., Goldenberg, M., and Cantor, C. (1983) *Cold Spring Harbor Symp. Quant. Biol.* **47,** 189–195.
2. Schwartz, D., and Cantor, C. (1984) *Cell* **37,** 67–75.
3. Carle, G., Frank, M., and Olson, M. (1986) *Science* **232,** 65–68.
4. Klotz, L., and Zimm, B. (1972) *Macromolecules* **5,** 471–481.
5. Kaback, D., and Davidson, N. (1980) *J. Mol. Biol.* **138,** 745–754.
6. Guo, X., Huff, E., and Schwartz, D. (1992) *Nature* **359,** 783–784.
7. Guo, X., Huff, E., and Schwartz, D. (1993) *J. Biomol. Struct. Dyn.* **11,** 1–10.
8. Schurr, J., and Smith, S. (1990) *Biopolymers* **29,** 1161–1165.
9. Smith, S., and Bendich, A. (1990) *Biopolymers* **29,** 1167–1173.
10. Doi, M., and Edwards, S. (1986) The Theory of Polymer Dynamics, Clarendon Press, Oxford.
11. de Gennes, P. (1979) Scaling Concepts in Polymer Physics, Cornell University Press, Ithaca.
12. Pascual-Leone, A., Grafman, J., and Hallet, M. (1994) *Science* **263,** 1287.
13. Graessley, W. (1982) *Adv. Polym. Sci.* **47,** 67–116.
14. Deutsch, J., and Madden, T. (1989) *J. Chem. Phys.* **90,** 2476–2485.
15. Duke, T., and Viovy, J. (1992) *Phys. Rev. Lett.* **68,** 542–545.
16. Perkins, T., Smith, D., and Chu, S. (1994) *Science* **264,** 819–822.
17. Volkmuth, W., Strick, T., Duke, T., Austin, R., and Cox, E. (1994) *Biophys. J.* **66,** A280.
18. Volkmuth, W., and Austin, R. (1992) *Nature* **358,** 600–602.
19. Lerman, L., and Frisch, H. (1982) *Biopolymers* **21,** 995–997.
20. Lumpkin, O., and Zimm, B. (1982) *Biopolymers* **21,** 2315–2316.
21. Schwartz, D., and Koval, M. (1989) *Nature* **338,** 520–522.
22. Zimm, B. (1988) *Phys. Rev. Lett.* **61,** 2965–2968.
23. Zimm, B. (1991) *J. Chem. Phys.* **94,** 2187–2206.
24. Smith, S., Aldridge, P., and Callis, J. (1989) *Science* **243,** 203–206.
25. Deutsch, J. (1988) *Science* **240,** 922–924.
26. Smith, S., Finzi, L., and Bustamante, C. (1992) *Science* **258,** 1122–1126.
27. Bustamante, C., Marko, J., Siggia, E., and Smith, S. (1994) *Science* **265,** 1599.
28. Rouse, P. (1953) *J. Chem. Phys.* **217,** 1272–1280.
29. Bird, R., Armstrong, R., and Hassager, O. (1977) Dynamics of Polymeric Liquids, John Wiley, New York.
30. Zimm, B. (1956) *J. Chem. Phys.* **24,** 269–278.
31. Schwartz, D. (1985) Ph.D. thesis (Columbia University).
32. Yanagida, M., Kroikawa, K., Hiraoka, Y., Matsumoto, S., Uemura, T., and Okada, S. (1986) Applications of Fluorescence in the Biomedical Sciences (Taylor, D., Ed.), pp. 321–345. Alan R. Liss, New York.
33. Rampino, N., and Chrambach, A. (1991) *Biopolymers* **31,** 1297–1307.
34. Gurrieri, S., Rizzarelli, E., Beach, D., and Bustamante, C. (1990) *Biochemistry* **29,** 3396–3401.
35. Perkins, T., Quake, S., Smith, D., and Chu, S. (1994) *Science* **264,** 822–826.
36. Link, A., and Olson, M. (1991) *Genetics* **127,** 681–698.
37. Podgornik, R., and Parseghian, V. (1990) *Macromolecules* **23,** 2265.
38. Yamakawa, H. (1971) Modern Theory of Polymer Solutions, Harper and Row, New York.
39. Fixman, M., and Kovac, J. (1973) *J. Chem. Phys.* **58,** 1564.
40. Fixman, M. (1966) *J. Chem. Phys.* **45,** 785–803.
41. Berry, G., and Casassa, E. (1970) *Macromolecular Reviews* **4,** 1–66.